J. Phys.: Condens. Matter **12** (2000) 9751–9760. Printed in the UK PII: S0953-8984(00)14813-1

In situ EXAFS and XANES measurements of the change in Ti coordination during the calcination of a $(TiO_2)_{0.18}(SiO_2)_{0.82}$ aerogel

D M Pickup†, G Mountjoy†, M A Holland†, G W Wallidge‡, R J Newport† and M E Smith‡

† School of Physical Sciences, University of Kent at Canterbury, Canterbury CT2 7NR, UK
‡ Department of Physics, University of Warwick, Coventry CV4 7AL, UK

Received 19 June 2000, in final form 20 September 2000

Abstract. The calcination of a $(TiO_2)_{0.18}(SiO_2)_{0.82}$ aerogel has been followed using *in situ* high-temperature Ti K-edge 'quick EXAFS' and XANES measurements. The results clearly show that the coordination of Ti in this material changes from a mixture of four- and sixfold to predominantly fourfold as the temperature is increased from ambient to 300 °C. The decrease in static disorder, as the environment of Ti converts to predominantly a single site, is such that the overall Debye–Waller factor for the Ti–O shell decreases markedly even as the temperature increases to 700 °C. Combined 'quick EXAFS' and XANES measurements are shown to be valuable tools for *in situ* studies of structural changes associated with thermal treatment of amorphous materials.

1. Introduction

Titania–silica mixed oxide materials, $(TiO_2)_x(SiO_2)_{1-x}$, have received much attention over recent years because their physical properties lend them to a number of technological uses. These materials have found use as ultra-low-thermal-expansion glasses [1], catalysts and catalyst supports [2] and thin films with tailored refractive indices [3]. The individual properties of titania–silica binaries depend on their chemical composition, homogeneity and texture. Some control over these characteristics is afforded by the chosen method of synthesis. Sol–gel synthesis from alkoxide precursors offers a simple and inexpensive low-temperature route to materials with a high degree of atomic mixing [1]. The exact conditions of synthesis also offer a degree of control over the pore sizes and surface areas of the resultant materials, two properties which are particularly important in terms of catalytic activity [4].

We have recently shown that the calcination of a $(TiO_2)_{0.18}(SiO_2)_{0.82}$ xerogel can be followed using *in situ* high-temperature x-ray diffraction measurements collected with a curved image-plate detector used in conjunction with a synchrotron radiation source [5]. The results indicate that in the unheated $(TiO_2)_{0.18}(SiO_2)_{0.82}$ xerogel the majority of Ti occupies sixfold sites with respect to oxygen; with heating these sixfold sites gradually convert to fourfold sites. By 310 °C, the majority of Ti is fourfold and can be considered as substituted into the silica network.

EXAFS and XANES have previously been demonstrated to be valuable techniques for determining titanium coordination numbers and environments in sol–gel derived $(TiO_2)_x(SiO_2)_{1-x}$ materials ([6], and references therein). In this paper, we describe the use of site specific, combined *in situ* high-temperature EXAFS and XANES to follow the calcination

0953-8984/00/479751+10$30.00

of a $(TiO_2)_{0.18}(SiO_2)_{0.82}$ aerogel. These measurements were made possible by the use of the 'quick EXAFS' (quEXAFS) scanning technique [7], which allows the collection of high-quality data in a fraction of the time required for conventional scanning.

2. Experimental details: sample preparation

The sample was prepared using the following precursors: tetraethyl orthosilicate, TEOS (Aldrich, 98%), and titanium (IV) isopropoxide, $Ti(OPr^i)_4$ (Aldrich, 97%). HCl was used as a catalyst to promote the hydrolysis and condensation reactions and isopropanol, IPA (Fluka, 99.5%) was used as a mutual solvent. All reagents were loaded in a dry box and transferred using syringes to avoid absorption of moisture from the atmosphere. The dry box used was a single-port type, connected to a vacuum pump and a cylinder of dry nitrogen. The alkoxide precursors were checked for hydrolysis using FTIR.

The preparation method used was that of Yoldas [8], which involves reacting $Ti(OPr^i)_4$ with a prehydrolysed solution of TEOS. The chosen prehydrolysis conditions were TEOS:IPA:H_2O in a 1:1:1 molar ratio in the presence of HCl (pH 1), stirring for two hours. The resulting sol was stirred for a few minutes before water was added slowly such that the overall water:alkoxide molar ratio (R) was 2. Stirring was continued until the sol had gelled, which took two days. The wet gel was dried from CO_2 by supercritical extraction at $>35\,^{\circ}C$ and >74 bar for 2 h [9]. The resultant aerogel had the nominal composition $(TiO_2)_{0.18}(SiO_2)_{0.82}$. It should be noted that this labelling of the sample only represents the composition after calcination to 700 °C: at lower temperatures the sample will contain unreacted alkoxide groups, solvent molecules and hydroxyl groups.

3. Experimental details: EXAFS and XANES measurements

The XAS (x-ray absorption spectroscopy) data were collected at the Ti K edge (4966 eV) in transmission mode on station 7.1 at the Daresbury Laboratory SRS using a Si [111] crystal monochromator and 70% harmonic rejection. Ionization chambers, filled with a mixture of Ar/He or Kr/He at appropriate partial pressures to optimize detector sensitivities, were placed in the beam path before and after the sample. The finely ground sample was diluted in boron nitride and pressed into a pellet. The concentration was adjusted to give a satisfactory edge jump and absorption. *In situ* heating of the sample was provided by a custom-made furnace fitted with polyimide windows. Calibration of the furnace revealed the temperature controller to be accurate to within $\pm 10\,^{\circ}C$.

Data acquisition was carried out in the 'quick EXAFS' mode (quEXAFS) [7] with each spectrum being the result of two 15 min scans. The quick EXAFS mode works by collecting data while the monochromator is moving with the counts from each segment of monochromator movement collected into one data point. With conventional EXAFS scanning the monochromator moves to each energy position and stops while the counts at that energy are collected. The quEXAFS method collects equivalent data in approximately one third of the time and is therefore particularly suited to *in situ* measurements.

4. Results and data analysis

A heuristic version of the equation for the interpretation of EXAFS data is

$$\chi(k) = \mathrm{AFAC} \sum_j \frac{N_j}{kR_j^2} |f(\pi, k, R_j)| e^{-2R_j/\lambda(k)} e^{-2\sigma_j^2 k^2} \sin(2kR_j + 2\delta(k) + \psi(k, R_j))$$

Table 1. Ti K-edge EXAFS derived structural parameters for reference compounds. The values in italics have been fixed. Note that N, R, A and R_{di} represent coordination number, interatomic distance, Debye–Waller factor and discrepancy index, respectively.

Sample	Shell	N	R (Å)	A (Å^2)	R_{di} (%)	Crystallographic data (Å) [11, 12]
TiO_2 rutile	Ti–O	*6*	1.92	0.012	41	6O × ~1.959
	Ti–Ti	*2*	2.96	0.012		2Ti × 2.959
	Ti–Ti	*8*	3.57	0.015		8Ti × 3.569
Ti-doped	Ti–O	*5*	1.88	0.021	44	~5O × 1.89
cristobalite	Ti–Ti	*1*	2.99	0.007		~1Ti × 2.959
(+some rutile)	Ti–Ti	*4*	3.56	0.012		~4Ti × 3.570

where $\chi(k)$ is the magnitude of the x-ray absorption fine structure as a function of the photoelectron wave vector $\boldsymbol{k}$. AFAC is the proportion of electrons that perform an EXAFS-type scatter. N_j is the coordination number and R_j is the interatomic distance for the jth shell. $\delta(k)$ and $\psi(k, R_j)$ are the phase shifts experienced by the photoelectron, $f(\pi, k, R_j)$ is the amplitude of the photoelectron backscattering and $\lambda(k)$ is the electron mean free path; these are calculated within EXCURV98 [10]. The Debye–Waller factor is $A = 2\sigma^2$ in EXCURV98.

The programs EXCALIB, EXBACK and EXCURV98 [10] were used to extract the EXAFS signal and analyse the data. Least-squares refinements of the structural parameters of our samples were carried out against the k^3 weighted $\chi(k)$. The parameters were obtained by fitting the EXAFS data over the range 3.70–12.0 Å^{-1} using the single-scattering approximation. Reasonable estimates of the errors are ±20% for the coordination numbers and ±0.02 Å for the nearest-neighbour distances. The results of the refinements are reported in terms of the discrepancy index, R_{di}:

$$R_{di} = \frac{\int |(\chi^T(k) - \chi^E(k))|k^3 \,\mathrm{d}k}{\int |\chi^E(k)|k^3 \,\mathrm{d}k} \times 100\%.$$

Reference materials were run in order to check the validity of our data analysis and also to allow refinement of AFAC. The references used were rutile, TiO_2, and a sample of cristobalite doped with 8 mol% Ti. Previously, powder x-ray diffraction (XRD) had shown the sample of Ti-doped cristobalite to contain a significant proportion of rutile (caused by phase separation during synthesis). The approximate amount of rutile present in the cristobalite sample was estimated by calculating the amount of Ti dissolved in the cristobalite structure from the modified positions of the cristobalite Bragg peaks in the XRD powder pattern [11]: the substitution of Si^{4+} ions by larger Ti^{4+} ions leads to a linear increase of the tetragonal unit cell constants. The present sample was calculated to contain ~4 mol% Ti dissolved in the cristobalite network, and hence the remaining Ti was assumed to be present as rutile. The results obtained from the analysis of the EXAFS data obtained from the reference materials are summarized in table 1. In these refinements, the coordination numbers were fixed at values consistent with the crystallographic data available [11, 12]. Reasonable agreement is obtained between the EXAFS and crystallographic structural parameters for rutile. The only noteworthy discrepancy is that between the value for the nearest-neighbour Ti–O distance; the EXAFS value is 0.04 Å too short. Part of the reason for this may be that in rutile there are two nearest-neighbour Ti–O distances present, a short distance of 1.948 Å and a longer distance of 1.980 Å. It seems that using a single-shell fit to model the EXAFS data in this region leads to a larger than expected error in the average Ti–O distance. Attempts to model the EXAFS

Table 2. Ti K-edge EXAFS derived structural parameters for $(TiO_2)_{0.18}(SiO_2)_{0.82}$ aerogel during calcination. Note that N, R, A and R_{di} represent coordination number, interatomic distance, Debye–Waller factor and discrepancy index, respectively. Reasonable estimates of the errors are ±20% for the coordination numbers and ±0.02 Å for the nearest-neighbour distances.

Temperature (°C)	N_{Ti-O}	R_{Ti-O} (Å)	A_{Ti-O} (Å^2)	R_{di} (%)
Ambient	5.3	1.83	0.028	29
100	4.6	1.81	0.021	26
200	4.6	1.80	0.018	27
300	4.3	1.80	0.014	27
400	4.1	1.80	0.011	23
500	4.1	1.80	0.012	26
600	3.9	1.80	0.011	26
700	3.8	1.80	0.010	27

Table 3. Heights of the Ti K-edge pre-peak for the reference materials and for the $(TiO_2)_{0.18}(SiO_2)_{0.82}$ aerogel *in situ* at various temperatures.

Sample	Temperature (°C)	Height of pre-edge peak ±4 (au)
TiO_2 rutile	Ambient	19
Ti-doped cristobalite (+some rutile)	Ambient	28
$(TiO_2)_{0.18}(SiO_2)_{0.82}$	Ambient	19
	100	23
	200	39
	300	46
	400	49
	500	54
	600	51
	700	46

data from rutile using two Ti–O nearest-neighbour shells resulted in meaningless values for the Debye–Waller factors.

The crystallographic parameters for the Ti doped cristobalite sample were calculated by treating the sample as a mixture of cristobalite and rutile with 50% of the Ti present as rutile, i.e. the average Ti site is five coordinate with an average Ti–O distance of 1.89 Å. There is good agreement between the EXAFS derived parameters from the cristobalite sample and those estimated from the crystallographic data. The large Debye–Waller factor for the Ti–O shell reflects the fact that two distinct Ti–O distances are present; a short distance of about 1.80 Å for the four-coordinate Ti substituted into the cristobalite structure and a longer distance of about 1.95 Å for the sixfold Ti present in the phase separated rutile component of this sample.

A value of 0.75 for AFAC was obtained from the analysis of the EXAFS data from the reference compounds; this value was used throughout the analysis of the *in situ* data from the $(TiO_2)_{0.18}(SiO_2)_{0.82}$ aerogel sample. The structural parameters obtained from the *in situ* EXAFS measurements taken during calcination are shown in table 2. Figures 1 and 2 show the EXAFS data and their Fourier transforms together with the calculated fits at two temperatures, 100 and 700 °C, respectively.

The XANES spectra were processed in the usual way [13] to obtain the absorbance, $\mu t = \ln(I_t/I_0)$, where I_0 and I_t are the incident and transmitted beam intensities, respectively.

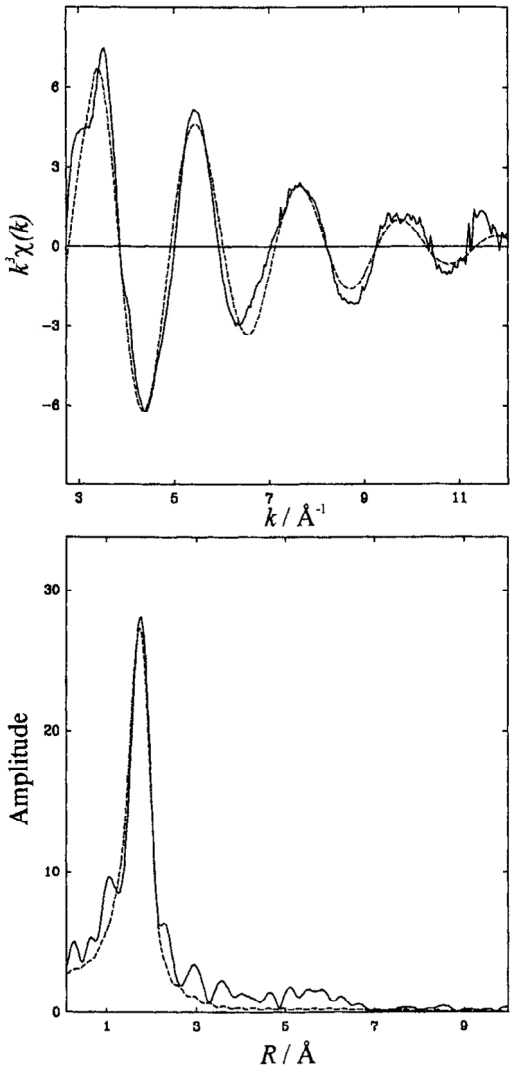

Figure 1. Ti K-edge EXAFS data for the $(TiO_2)_{0.18}(SiO_2)_{0.82}$ aerogel collected *in situ* at 100 °C: k^3 weighted EXAFS (top) and Fourier transform (bottom). Experimental data, solid line, and theoretical fit, dotted line.

The pre- and post-edge backgrounds were then fitted to obtain normalized absorbance, $\chi(E) = (\mu t(E) - \mu t_{\text{pre}})/(\mu t_{\text{post}} - \mu t_{\text{pre}})$. The height of the pre-edge peak was measured for each spectrum and the results tabulated in table 3.

The height of the pre-edge peak which occurs at the Ti K-edge yields information about the Ti coordination [14]. This pre-edge peak is assigned to transitions to T_{2g} states [15] and occurs due to pd mixing [16]. Since the extent of pd mixing depends inversely on the degree of centrosymmetry around the Ti atom, the pre-edge peak intensity increases as the coordination changes from octahedral to tetrahedral. Here we use the height of the pre-edge peak to obtain a qualitative estimate the relative amounts of octahedral and tetrahedral Ti present in the aerogel at each temperature.

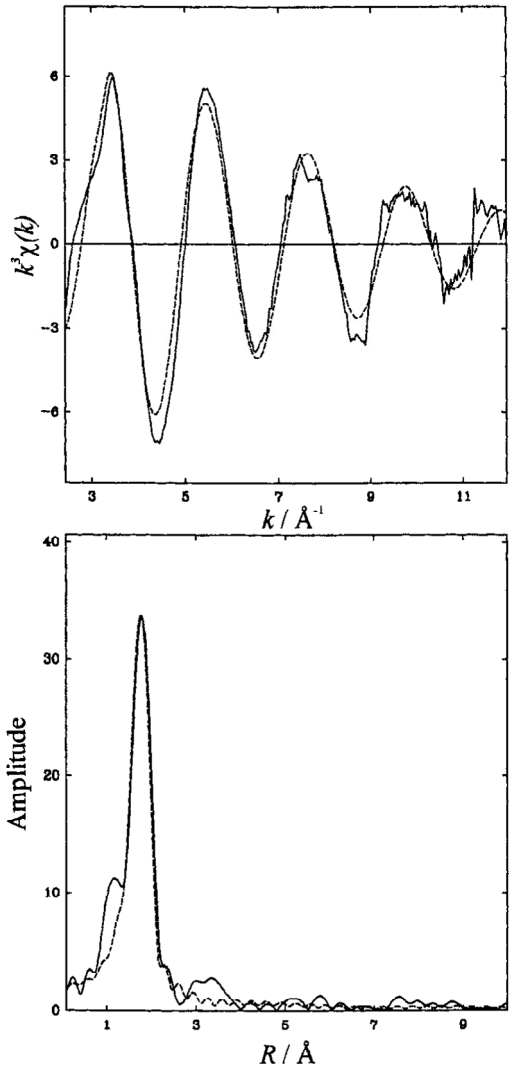

Figure 2. Ti K-edge EXAFS data for the $(TiO_2)_{0.18}(SiO_2)_{0.82}$ aerogel collected *in situ* at 700 °C: k^3 weighted EXAFS (top) and Fourier transform (bottom). Experimental data, solid line, and theoretical fit, dotted line.

5. Discussion

The results in table 2 clearly show a decrease in Ti–O coordination number and the associated bond distance during calcination of the $(TiO_2)_{0.18}(SiO_2)_{0.82}$ aerogel. These results are entirely consistent with those of our previous XRD study [5], i.e. by the time the sample has reached 300–350 °C, virtually all the sixfold Ti has been converted to fourfold Ti. This coordination is then maintained through further heating up to 700 °C. The fourfold Ti has a Ti–O bond length of ~1.80 Å, which is close to the Si–O bond length of 1.62 Å, thus allowing substitution of Ti into tetrahedral sites within the silica network. The mechanism of this substitution is thought to involve the loss of water ligands from the Ti coordination sphere during the early stages of heating (up to 300 °C). Evidence for this mechanism comes from earlier

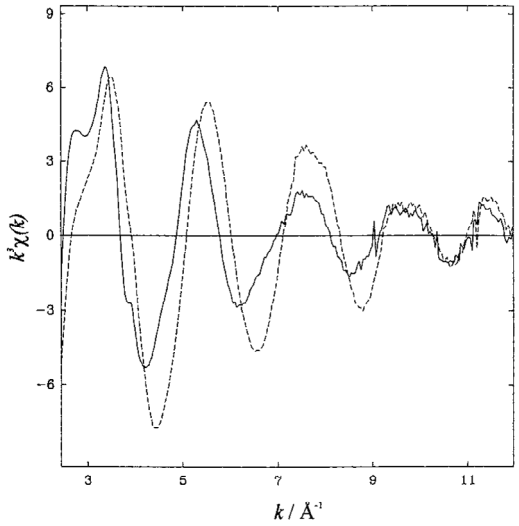

Figure 3. Comparison of the Ti K-edge k^3 weighted EXAFS data for the $(TiO_2)_{0.18}(SiO_2)_{0.82}$ aerogel at ambient temperature (solid line) and *in situ* at 300 °C (dotted line).

in situ XANES measurements [17], which demonstrated that the change from six- to fourfold Ti coordination is reversible upon re-exposure to ambient conditions up to temperatures of 250 °C. *Ex situ* XANES results obtained from the same study showed that further heating causes relaxation of the silica network and the change to fourfold Ti coordination to become irreversible.

The most interesting feature of these results is that the Debye–Waller factor for the Ti–O nearest-neighbour shell actually decreases as the sample is heated. Figure 3 illustrates this point, showing the reduction in the damping of the EXAFS oscillations at high k as the temperature is raised from ambient to 300 °C. This point can be further investigated by examining the Debye–Waller factors more closely. There are two contributions to these temperature factors ($A = 2\sigma^2$):

$$A_{\text{total}} = A_{\text{thermal}} + A_{\text{static}}.$$

The thermal contribution can be estimated from the vibrational frequency of the bond in question by assuming it can be modelled by a diatomic harmonic oscillator [18]:

$$\sigma^2_{vib} = \frac{h}{8\pi^2\mu\nu}\coth\left(\frac{h\nu}{2kT}\right)$$

where μ is the reduced mass, T is the temperature and ν is the vibrational frequency. In this case the thermal contribution to the Debye–Waller factor can be broken down into two terms which arise from the presence of two Ti sites; A_4, being defined as the contribution from fourfold Ti and A_6 the contribution from sixfold Ti. Estimates of A_4 and A_6 were calculated using the frequencies derived by Kusabiraki [19] for TiO_4 (940 cm^{-1}) and TiO_6 (570 cm^{-1}) sites in TiO_2–Na_2O–SiO_2 glasses. The results of these calculations are presented in table 4. This analysis can be taken further by estimating the proportion of fourfold Ti, x, from the average Ti–O coordination number, N_{Ti-O}, derived from the EXAFS results using the equation $x = (6 - N_{Ti-O})/2$. Using the values of x calculated at each temperature, estimates

Table 4. Experimental and calculated Debye–Waller factors at various temperatures for the Ti–O shell during calcination of the $(TiO_2)_{0.18}(SiO_2)_{0.82}$ aerogel.

Temperature (°C)	Proportion of fourfold Ti, x	Calculated Debye–Waller factors			Experimental Debye–Waller factors
		A_4 (Å^2)	A_6 (Å^2)	A_{total} (Å^2)	A_{total} (Å^2)
Ambient	0.35	0.003	0.006	0.014	0.028
100	0.70	0.003	0.006	0.015	0.021
200	0.70	0.003	0.007	0.016	0.018
300	0.85	0.004	0.008	0.012	0.014
400	0.95	0.004	0.009	0.007	0.011
500	0.95	0.004	0.010	0.008	0.012
600	1.00	0.005	0.011	0.005	0.011
700	1.00	0.005	0.012	0.005	0.010

of the overall Debye–Waller factors can be calculated using the following equation:

$$A_{\text{total}} = \frac{[4xA_4 + 6(1-x)A_6]}{(6-2x)} + \frac{[48(\Delta R)^2 x(1-x)]}{(6-2x)^2}$$

where ΔR is the difference between the Ti–O bondlengths for sixfold and fourfold Ti; in this case 1.95 Å − 1.80 Å = 0.15 Å. The first term in the square brackets is simply a weighted average of the two thermal contributions, A_4 and A_6, and the second term is a static term arising from the presence of two mean distances. The results of these calculations are compared with the experimental total Debye–Waller factors in table 4. Also presented are the estimates of x used in the calculations. There are two points to mention concerning the values of x. Firstly, in the cases where the EXAFS data analysis gave values of N_{Ti-O} less than 4 the calculated values of x are greater than 1. This is not physically possible, and for this reason we imposed an upper limit of 1 for x. Secondly, it should be noted that values of x could also have been calculated from the EXAFS derived R_{Ti-O} values. However, it has previously been shown [6] that sixfold Ti has an asymmetric distribution of bond lengths, which may give a shorter mean bond length than expected (there is little variation in the bond length for fourfold Ti). This situation complicates the interpretation of the EXAFS bond lengths obtained by fitting a single Ti–O shell and makes estimation of the relative proportions of four- and sixfold Ti difficult.

The agreement between the calculated and experimental Debye–Waller factors is reasonable considering the error bars associated with the calculated values and also the assumptions made in the calculations. The values of x used in the calculations are only very rough estimates because of the relatively large errors associated with coordination numbers obtained from EXAFS measurements. Also the calculation used does not account for any static disorder within the two Ti sites. It has already been mentioned that there is an expected spread of Ti–O bond lengths for sixfold Ti and this is probably the cause of the largest discrepancy between the room-temperature values of 0.014 and 0.028 Å^2 for the calculated and experimental Debye–Waller factors respectively. In general, the exclusion of static disorder within the individual Ti sites will always lead to the calculated values being lower than the experimental ones. However, the main point is that both the calculated and experimental Debye–Waller factors exhibit the same trend of decreasing with increasing temperature. This decrease occurs for two reasons. Firstly, the static disorder is reduced considerably as sixfold Ti is converted to fourfold Ti, leading to a strong predominance of only the fourfold site by 300 °C. Secondly, the increasing thermal contribution to the Debye–Waller factor due to the increase in temperature is off-set by the fact that as the proportion of sixfold Ti is reduced, so is the contribution to

the thermal term from A_6. This reduces the increase in the total thermal Debye–Waller factor because A_6 is always greater than A_4 due to the lower frequency of the Ti–O vibrations in the sixfold site. The decrease in the experimental Debye–Waller factor is greatest up to 300 °C, reflecting that this is the temperature range where the most structural change is occurring within the sample as water ligands are driven off.

The XANES results shown in table 3 support the conclusions drawn from the analysis of the EXAFS data. As discussed earlier, the height of the pre-edge peak gives a guide to the amount of Ti present in tetrahedral sites. There is a sharp increase in the peak height between room temperature and 300 °C as octahedral Ti sites are reversibly converted into tetrahedral Ti sites by the loss of water ligands. By comparison with the result for the Ti doped cristobalite sample, which has been estimated to contain approximately a 50/50 mixture of octahedral and tetrahedral Ti, it is possible to say that by 200 °C at least half of the titanium is present in tetrahedral sites. This estimate agrees well with that of 70% fourfold Ti at 200 °C obtained from the EXAFS data (see table 4). Above 300 °C there is no significant increase in the height of the pre-edge peak with temperature, indicating that the proportion of Ti in tetrahedral sites is not increasing, although the nature of these sites is changing due to relaxation of the network.

6. Conclusions

The calcination of a $(TiO_2)_{0.18}(SiO_2)_{0.82}$ aerogel has been followed using *in situ* high-temperature quEXAFS and XANES measurements. The results clearly show that the coordination of Ti changes from a mixture of four- and sixfold to predominantly fourfold as the temperature is increased from ambient to 300 °C. The decrease in static disorder due to the change in Ti coordination is such that the Debye–Waller factor for the Ti–O shell decreases even as the temperature increases to 700 °C. This shows that quEXAFS and XANES are valuable, and complementary, techniques for *in situ* studies of the structural changes in amorphous materials.

Acknowledgments

The EPSRC is thanked for its support of the characterization of sol–gel produced materials through grant GR/L28647 and for the funding of Dr G Mountjoy through grant GR/K95987. Dr N Chinnery is thanked for his help with the data collection.

References

[1] Brinker C J and Scherer G W 1990 *Sol–Gel Science: the Physics and Chemistry of Sol–Gel Processing* (San Diego, CA: Academic)
[2] Itoh M, Hattori H and Tanabe K J 1974 *J. Catal.* **35** 225
[3] Schultz P C and Smyth H T 1972 *Amorphous Materials* ed E W Douglas and B Ellis (London: Wiley)
[4] Holland M A, Pickup D M, Mountjoy G, Tsang E S C, Wallidge G W, Smith M E and Newport R J 2000 *J. Mater. Chem.* **10** 2495
[5] Pickup D M, Mountjoy G, Roberts M A, Wallidge G, Newport R J and Smith M E 2000 *J. Phys.: Condens. Matter* **12** 3512
[6] Mountjoy G, Pickup D M, Wallidge G W, Anderson R, Cole J M, Newport R J and Smith M E 1999 *Chem. Mater.* **11** 1253
[7] Murphy L M, Dobson B R, Neu M, Ramsdale C A, Strange R W and Hasnain S S 1995 *J. Synchrotron Radiat.* **2** 64
[8] Yoldas B E 1980 *J. Non-Cryst. Solids* **38** 81
[9] Tamon H, Sone T and Okazaki M 1997 *J. Colloid Interface Sci.* **188** 162

[10] Binstead N, Campbell J W, Gurman S J and Stephenson P C 1991 *EXAFS Analysis Programs* (Warrington: Daresbury Laboratory)
[11] Evans D L 1982 *J. Non-Cryst. Solids* **52** 115
[12] Abrahams S C and Bernstein J L 1971 *J. Phys. Chem.* **55** 3206
[13] Bianconi A 1987 *X-Ray Absorption: Principles, Applications, Techniques of EXAFS, SEXAFS and XANES* ed D C Koninbsberger and R Prins (New York: Wiley) ch 11
[14] Farges F, Brown G E and Rehr J J 1997 *Phys. Rev.* B **56** 1807
[15] Babonneau F, Doeuff S, Leaustic A, Sanchez C, Cartier C and Verdaguer M 1988 *Inorg. Chem.* **27** 3166
[16] Grunes L A 1983 *Phys. Rev.* B **27** 2111
[17] Mountjoy G, Pickup D M, Wallidge G W, Cole J M, Newport R J and Smith M E 1999 *Chem. Phys. Lett.* **304** 150
[18] Teo B K 1986 *EXAFS Basic Principles and Data Analysis* (New York; Springer)
[19] Kusabiraki K 1986 *J. Non-Cryst. Solids* **79** 208